



**HAL**  
open science

# Chemistry in the Molten State: Opportunities for Designing and Tuning the Emission Properties of Halide Perovskites

Feten Hleli, Nicolas Mercier, Maroua Ben Haj Salah, Magali Allain, Nabil Zouari, Florian Massuyeau, Romain Gautier

► **To cite this version:**

Feten Hleli, Nicolas Mercier, Maroua Ben Haj Salah, Magali Allain, Nabil Zouari, et al.. Chemistry in the Molten State: Opportunities for Designing and Tuning the Emission Properties of Halide Perovskites. *Inorganic Chemistry*, 2023, 62 (35), pp.14252-14260. 10.1021/acs.inorgchem.3c01566 . hal-04214987

**HAL Id: hal-04214987**

**<https://hal.science/hal-04214987>**

Submitted on 10 Nov 2023

**HAL** is a multi-disciplinary open access archive for the deposit and dissemination of scientific research documents, whether they are published or not. The documents may come from teaching and research institutions in France or abroad, or from public or private research centers.

L'archive ouverte pluridisciplinaire **HAL**, est destinée au dépôt et à la diffusion de documents scientifiques de niveau recherche, publiés ou non, émanant des établissements d'enseignement et de recherche français ou étrangers, des laboratoires publics ou privés.

# Chemistry in the Molten State: Opportunities for Designing and Tuning the Emission Properties of Halide Perovskites

*Feten Hleli,<sup>a,b</sup> Nicolas Mercier,<sup>a\*</sup> Maroua Ben Haj Salah,<sup>a</sup> Magali Allain,<sup>a</sup> Nabil Zouari,<sup>b</sup>*

*Florian Massuyeau,<sup>c</sup> Romain Gautier<sup>c</sup>*

<sup>a</sup> *MOLTECH-Anjou, UMR-CNRS 6200, Université d'Angers, 2 Bd Lavoisier, 49045 Angers, France.*

<sup>b</sup> *Laboratoire Physico-chimie de l'Etat Solide, Département de Chimie, Faculté des Sciences de Sfax, B.P. 1171, 3000 Sfax, Université de Sfax, Tunisia.*

<sup>c</sup> *Nantes Université, CNRS, Institut des Matériaux de Nantes Jean Rouxel, IMN, F-44000 Nantes, France*

KEYWORDS. halide perovskite; luminescence; congruent melting; solid solutions; molten state synthesis.

## ABSTRACT

A series of monolayered lead halide hybrid perovskites  $(\text{HO}_2\text{C}(\text{CH}_2)_{n-1}\text{NH}_3)_2\text{PbX}_4$  named  $(\text{C}_n)_2\text{PbX}_4$  ( $n= 4-6$ ,  $\text{X}=\text{Cl}, \text{Br}$ ) exhibiting low congruent melting temperature  $-T_m$ - ( $T_m= 130\text{ }^\circ\text{C}$  for  $(\text{C}_4)_2\text{PbBr}_4$ ), high stability in the molten state and whitish type emission, are reported. From the synthesis in the molten state, rare solid solutions of mixed organic cations  $(\text{C}_{n(1-x)}\text{C}_{n'x})_2\text{PbX}_4$  ( $n, n'= 4-6$ ;  $\text{X}=\text{Cl}, \text{Br}$ ;  $0\leq x\leq 1$ ) as well as solid solutions of mixed halides  $(\text{C}_n)_2\text{Pb}(\text{X}_{1-y}\text{X}'_y)_4$  ( $n= 4-6$ ;  $\text{X}, \text{X}'=\text{Cl}, \text{Br}$ ;  $0\leq y\leq 1$ ) have been prepared and characterized (thermal behaviour, PXRD, photoluminescence properties). The impact of substitutions is significant on thermal properties, lowering  $T_m$  down to  $100\text{ }^\circ\text{C}$  for  $(\text{C}_4)_2\text{Pb}(\text{Br}_{0.25}\text{Cl}_{0.75})_4$ . The emission properties are slightly tuned in the case of mixed organic cations systems, whereas modifications are more dramatic in the case of mixed halides systems, leading to emission properties through the entire visible region. These results illustrate the great opportunities offered by the congruent melting properties of halide perovskites allowing syntheses in the molten state.

## INTRODUCTION

Since a decade, halide perovskites (HP) are rock-star semiconducting materials, showing high potential for photovoltaic (Perovskite solar Cell -PSC- technology)<sup>1-3</sup> and lighting (Perovskite Light Emitting Devices -PeLED-) applications.<sup>4-6</sup> 2D (two dimensional) hybrid perovskites, or layered perovskites, are materials based on perovskite layers separated by organic cations.<sup>7-9</sup> The inorganic layers consist of corner-sharing  $B^{(II)}X_6$  (B: Pb, Sn,..; X= halide) octahedra extending along two directions of space. The main family of layered perovskites is the Ruddlesden-Popper (RP) one having the formula  $(A)_2(A')_{n-1}B^{(II)}_nX_{3n+1}$  where  $A^+$  is a large size cation separating perovskite layers, while the small size cation  $A^{+'}$  is included within the perovskite sheet ( $n \geq 2$ ). For solar cells application, the most interesting 2D perovskites are multi-layered perovskites ( $n > 2$ ) which have a good absorption in the all visible range.<sup>10-12</sup> On the other hand, monolayered perovskites  $(A)_2BX_4$  ( $n = 1$ ) appear very interesting materials for narrow or broad band emission properties.<sup>13-15</sup>

While the preparation of single crystals and powders of halide perovskites is mainly achieved from solutions, solvent-free methods would offer real advantages since they are greener routes and can make it possible to obtain compounds with a defined composition. Solid-state processes (ball-milling,..) represent the main solvent-free method, mainly applied to 3D inorganic halide perovskites, even if some 2D HP have been also prepared.<sup>16</sup> Recently, a solvent-free process has been proposed consisting of a liquid polyiodide resulting from the mixing of methylammonium iodide (MAI) and iodine powders, in which metallic lead is added, finally leading to the formation of  $MAPbI_3$ .<sup>17</sup> If 3D inorganic halide perovskites can exhibit congruent melting at high temperatures,<sup>18</sup> most of the 3D and 2D organic-inorganic halide perovskites decompose before melting, and only a few examples of  $(A)_2BX_4$  compounds exhibiting congruent melting (melting

without decomposition) had been reported : (2-FPEA)SnI<sub>4</sub> (2-FPEA= 2-fluorophenethylammonium; T<sub>m(melting)</sub>= 174 °C -first report, 2002-),<sup>19</sup> (A)<sub>2</sub>PbI<sub>4</sub> (A: phenylethylammonium derivatives, T<sub>m</sub> around 200 °C),<sup>20</sup> and (1Me-ha)PbI<sub>4</sub> (1-Me-ha = 1-methyl-hexylammonium, T<sub>m</sub>= 171 °C).<sup>21</sup> Very recently, we discovered that (C4)<sub>2</sub>PbI<sub>4</sub> (C<sub>4</sub>= HO<sub>2</sub>C(CH<sub>2</sub>)<sub>3</sub>NH<sub>3</sub><sup>+</sup> = 4-ammoniumbutyric acid) exhibits a record T<sub>m</sub> of 126°C and is stable in the molten state a few minutes which allowed the preparation of the n= 2 RP compound (C4)<sub>2</sub>MAPb<sub>2</sub>I<sub>7</sub> by reaction of (C4)<sub>2</sub>PbI<sub>4</sub> in the molten state and MAPbI<sub>3</sub> in the solid state.<sup>22</sup> Congruent melting of halide perovskites offers two main opportunities. First, these materials can be prepared as thin films by a solvent-free process, as demonstrated by D.B. Mitzi.<sup>19-21</sup> Second, the molten state could allow the synthesis of new phases, or doping, a well-known strategy to tune the emission properties of halide perovskites.<sup>23,24</sup> The synthesis, crystal structure and white light emission of the bromide perovskite (C4)<sub>2</sub>PbBr<sub>4</sub> were recently reported in 2017 but no emission/excitation spectrum was provided.<sup>25</sup> Recently we reported a complete study of its emission properties as well as the properties of mechanochromic luminescence of a composite consisting on a mixture of this 2D perovskite and the 3D compound (CH<sub>3</sub>NH<sub>3</sub>)PbBr<sub>3</sub>.<sup>26</sup>

In this context, we were interested in the opportunities to design new compositions and to tune the emission properties of 2D halide perovskites exhibiting congruent melting by carrying out chemistry in the molten state. We first prepared a series of monolayered halide perovskites based on linear amino acid type cations HO<sub>2</sub>C(CH<sub>2</sub>)<sub>n-1</sub>NH<sub>3</sub><sup>+</sup> (named C<sub>n</sub>, n= 4-6): (C<sub>n</sub>)<sub>2</sub>PbX<sub>4</sub> (X= Cl, Br). It is important to note that some of these compounds were already reported (n=4, X= Br;<sup>25</sup> n= 5, X= Cl, Br),<sup>27</sup> the bromide perovskites exhibiting a quite strong whitish emission with a main blue component while the chloride perovskite has a weak broad band emission. Then, from synthesis in the molten state, we prepared two types of series of solid solutions: i) rare solid

solutions of mixed organic cations  $(C_{n_{1-x}Cn'_x})_2PbX_4$  ( $n, n' = 4-6$ ;  $X = Cl, Br$ ;  $0 \leq x \leq 1$ ) and ii) solid solutions of mixed halides  $(Cn)_2Pb(X_{1-x}X'_x)_4$  ( $n = 4-6$ ;  $X, X' = Cl, Br$ ;  $0 \leq x \leq 1$ ). The powder X-ray diffraction (PXRD) analyses first allowed to define the  $x$  ranges of these solid solutions (full range for mixed halides, partial ones in the case of mixed organic cations) while differential scanning calorimetry (DSC) measurements revealed that all materials exhibit congruent melting, also showing that halide substitutions has a noticeable impact on thermal properties, lowering  $T_m$  down to 100 °C for  $(C4)_2Pb(Br_{0.75}Cl_{0.25})_4$ . Finally, the emission properties will be reported highlighting how the organic cations or halides substitutions tune both the intensity and color of emission.

## EXPERIMENTAL SECTION

**Synthesis and characterizations.** Crystals of  $(C6)_2PbBr_4$  have been obtained by liquid-gas diffusion method. Crystals of  $(Cn)_2PbCl_4$  ( $n=4, 6$ ) have been synthesized by evaporation and cooling down: the precursors  $PbCl_2$  and  $NH_2(CH_2)_{n-1}CO_2H$  are poured into concentrated HCl so that their concentration is greater than their solubility limit at room temperature. The heterogeneous solution is then heated to boiling in order to completely dissolve the precursors, while the solvent is partially eliminated by evaporation. Once the solution is homogeneous, a cooling down to room temperature allows the crystallization of perovskites. Crystallized powders of  $(C4)_2PbCl_4$  and  $(C6)_2PbX_4$  ( $X = Cl, Br$ ) as well of the three known perovskites  $(C4)_2PbBr_4$ <sup>25</sup> and  $(C5)_2PbCl_4$  ( $X = Br, Cl$ )<sup>27</sup> have been synthesized by a fast precipitation method (see details of all syntheses in Table S1). X-Ray powder diffraction (XRPD) analysis which was performed on a D8 Bruker diffractometer (Cu  $K\alpha$ ) equipped with a linear Vantec super speed detector, confirmed the phase purity, as all observed reflections could be indexed in the unit cell obtained from single crystal X-ray diffraction experiments (Figures S1-6).

The solid solutions  $(\text{Cn}_{1-x}\text{Cn}'_x)_2\text{PbBr}_4$  (where  $n, n' = 4-6$  and  $n \neq n'$ ) and  $(\text{Cn})_2\text{Pb}(\text{Br}_{1-x}\text{Cl}_x)_4$  have been prepared as follows: the solids  $(\text{Cn})_2\text{PbBr}_4$  and  $(\text{Cn}')_2\text{PbBr}_4$  or  $(\text{Cn})_2\text{PbBr}_4$  and  $(\text{Cn})_2\text{PbCl}_4$  are mixed, heating up to the molten state, keeping in the molten state a few minutes before cooling down to RT (see details of all syntheses in Tables S2-3).

The Differential scanning calorimetry (DSC) analyses of all compounds were performed using a TA instrument DSC Q20 in the temperature range 25-200 °C. The crystalline samples were placed in aluminium crucibles that were heated at scanning rate (10 K  $\text{mn}^{-1}$ ) under flowing nitrogen at atmospheric pressure.

**Single crystal X-ray crystallography.** X-ray diffraction data were collected on a Rigaku Oxford Diffraction diffractometer equipped with Atlas CCD detector and micro-focus  $\text{Cu-K}_\alpha$  radiation ( $\lambda = 1.54184 \text{ \AA}$ ) for  $(\text{C4})_2\text{PbCl}_4$  and  $(\text{C6})_2\text{PbBr}_4$  and on a Bruker D8 Quest diffractometer equipped with a PHOTON III detector and micro-focus  $\text{Mo-K}_\alpha$  radiation ( $\lambda = 0.71073 \text{ \AA}$ ) for  $(\text{C6})_2\text{PbCl}_4$ . Intensities were corrected for Lorentz-polarization effects, as well as for absorption effect (gaussian method using CrysAlisPro program -CrysAlisPro, Rigaku Oxford Diffraction, V1.171.41.118a, 2021 or multiscan method using SADABS.<sup>28</sup> The structures were solved using SHELXT program, and refined by full matrix least-squares routines against  $F^2$  using SHELX programs (G. M. Sheldrick, SHELXT 2018/2 and SHELXL 2019/3). All non-H atoms were refined anisotropically. The hydrogen atoms were treated with a riding model except for the H atom on the hydroxyl group which were first placed at calculated position taking into account the local electron density and the orientation of the molecules and then fixed with HFIX constraint for the convergence of the refinement. Many restraints on the distances and angles of the organic molecules were applied to be in agreement with the geometry of such molecules and dynamic disorder of the organic cations were treated if necessary. A summary of crystallographic data and

refinement results are listed in Tables S4-6. A complete list of crystallographic data, along with the atomic coordinates, the anisotropic displacement parameters and bond distances and angles are given as CIF file. CCDC Numbers 2256357 for  $(C6)_2PbBr_4$ , 2256358 for  $(C4)_2PbCl_4$  and 2256359 for  $(C6)_2PbCl_4$  contains the supplementary crystallographic data for this paper. These data are provided free of charge by The Cambridge Crystallographic Data Centre.

**Optical properties.** Photoluminescence experiments have been achieved on a Fluorolog-3 from Horiba, equipped with double-grating monochromators in excitation and emission and a 450W Xenon lamp. Photoluminescence quantum yield are calculated by adding a QuantaPhi accessory on the Fluorolog-3.

## RESULTS AND DISCUSSION

### Layered perovskites $(Cn)_2PbX_4$ ( $n=4-6$ ; $X= Cl, Br$ ).

The synthesis of the layered perovskites  $(Cn)_2PbX_4$  ( $n=4-6$ ;  $X= Cl, Br$ ) was carried in solution, either from liquid-gas diffusion methods or from evaporation and cooling down of solutions containing reagents and a few drops of acid (see experimental part). The comparison of experimental PXRD and calculated ones from single crystal X-ray data of  $(C4)_2PbBr_4$ ,<sup>25</sup>  $(C5)_2PbX_4$  ( $X= Cl, Br$ ),<sup>27</sup> and  $(C4)_2PbCl_4$  and  $(C6)_2PbX_4$  ( $X= Cl, Br$ ) (current work) shows that all materials have been obtained as pure phases (Figures S1-6). DSC experiments (heating and cooling steps) reveal reversible transitions in the range 147°C-211°C (Figure 1a and Figures S7-11) assigned to congruent melting processes which is confirmed by a visual examination of samples on a heating plate or using a Kofler bench. Figure 1a shows the DSC curve of  $(C4)_2PbBr_4$  as well as photos of the sample before heating, after melting and after recrystallization. Besides the 147 °C endothermic peak (melting), another reversible transition

around 73°C is detected certainly corresponding to structural changes, as also observed for (C5)<sub>2</sub>PbX<sub>4</sub> (X= Cl, Br) (Figures S8-S9). The melting temperatures (T<sub>m</sub>) increase when the length of the carbon chain increases, from 147°C for (C4)<sub>2</sub>PbBr<sub>4</sub> to 211°C for (C6)<sub>2</sub>PbBr<sub>4</sub> (157°C for (C5)<sub>2</sub>PbBr<sub>4</sub>) in the bromide series and from 148°C for (C4)<sub>2</sub>PbCl<sub>4</sub> to 212°C for (C6)<sub>2</sub>PbCl<sub>4</sub> (160°C for (C5)<sub>2</sub>PbBr<sub>4</sub>) for the chloride series, also meaning that melting temperatures are roughly similar whatever the halide nature for a given C<sub>n</sub> cation (Figure S12). In order to evaluate the stability of these perovskites in the molten state, powder samples are heated and as soon as melting is reached, they are left for a certain time (t) at this temperature, taken off the heating system, then naturally cooled down to room temperature. Figure 1b shows several room-temperature PXRD patterns of a (C4)<sub>2</sub>PbBr<sub>4</sub> sample previously hold in the molten state from t=0 to t= 30 min. For PXRD of samples from “t=0” to “t= 15 min”, only diffraction lines corresponding to the expected n= 1 perovskite are observed while for a longer time, a decomposition occurs as highlighted by new diffraction lines assigned to PbBr<sub>2</sub>. It appears that the stability in the molten state in ambient air of bromide compounds ((C<sub>n</sub>)<sub>2</sub>PbBr<sub>4</sub>) are much greater than the stability of the iodide perovskite (C4)<sub>2</sub>PbI<sub>4</sub> (t ≈15 min for bromides -see also Figure S13- vs a few minutes for the iodide perovskite<sup>26</sup>).

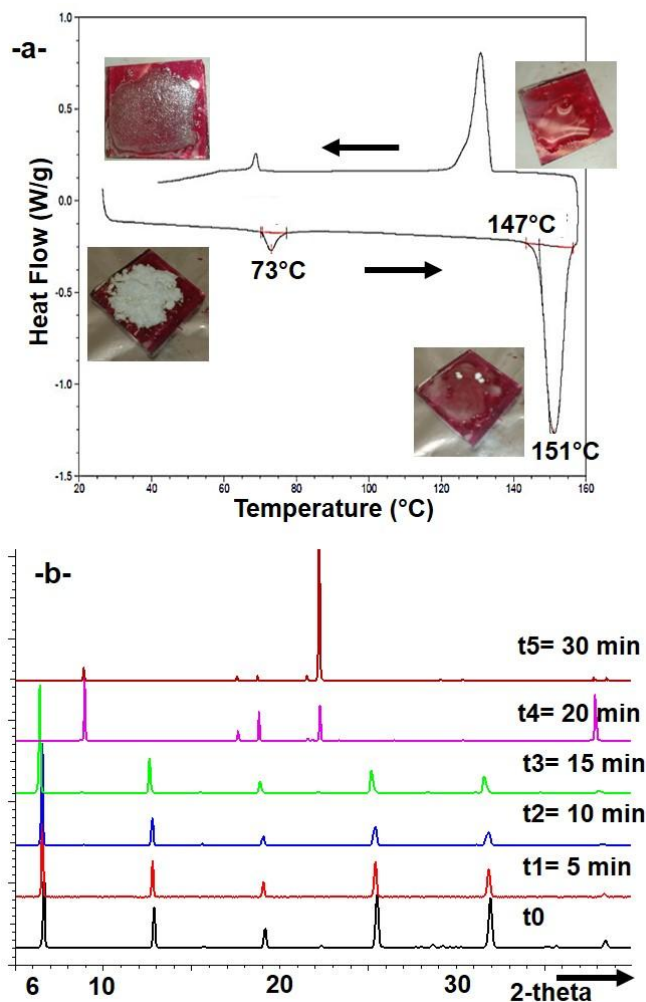


**Figure 1.** Differential scanning calorimetry (heating and cooling) of  $(C_4)_2PbBr_4$  and photos of a powder sample before heating, after melting and after recrystallization (a); room temperature PXRD patterns of a sample of  $(C_4)_2PbBr_4$  previously hold at 150 °C during  $t=0$  min to  $t=30$  min, showing that the compound is stable in the molten state up to 15 min of heating while a decomposition takes place beyond  $t=15$  min (b).

The Figure 2 shows selected views of the crystal structures of the layered perovskites  $(C_n)_2PbX_4$  ( $n=4-6$ ;  $X=Cl, Br$ ). While both structures based on  $C_5^+$  cations and the one of  $(C_4)_2PbBr_4$  were known, the other three are reported in this study (Tables S4-6 and cif in SI). The interlayer distance between two consecutive perovskite layers clearly increases when the number of carbon atoms of the organic cations increases for both the bromide and chloride series (for example from 14.2 Å ( $C_4$ ), 16.0 Å ( $C_5$ ) to 17.4 Å for the bromide series, Figure S14). Organic sheets separating perovskites layers are based on two sub-layers of molecules, and we notice that in all structures two carboxylic groups of two adjacent molecules interact through strong hydrogen

bonding leading to supramolecular dications  $[\text{NH}_3(\text{CH}_2)_{n-1}\text{CO}_2\text{H}\dots\text{HO}_2\text{C}(\text{CH}_2)_{n-1}\text{NH}_3]^{2+}$ . The broad band emission of some layered perovskites are assigned to exciton self-trapping (STE). This could occur when strong deformations of the perovskite network involve strong coupling between excitons and the lattice. Deformations of the inorganic lattice include octahedron distortions, in-plane distortions (rotation of octahedra in the layer plane involving Pb- $X_{\text{shared}}$ -Pb bond angle  $<180^\circ$ ) and out-of-plane distortions (tilt of octahedra relatively to layer planes -angle between the  $X_{\text{apical}}-X_{\text{apical}}$  line and the line perpendicular to layer  $> 0^\circ$ ). The out-of-plane distortions seem to have the main role involving broad band emission.<sup>25</sup> All six structures of this study roughly display the same structural features : polyhedra almost regular (in particular with similar bond distances within 2.82-2.89 Å range ((C6)<sub>2</sub>PbCl<sub>4</sub>); 2.84-2.89 Å ((C5)<sub>2</sub>PbCl<sub>4</sub>); 2.79-2.92 Å ((C4)<sub>2</sub>PbCl<sub>4</sub>); 2.97-3.00 Å ((C6)<sub>2</sub>PbBr<sub>4</sub>); 2.97-3.02 Å ((C5)<sub>2</sub>PbBr<sub>4</sub>); 2.93-3.02 Å ((C4)<sub>2</sub>PbBr<sub>4</sub>)), similar in-plane distortions (minimum angle of 147° ((C6)<sub>2</sub>PbCl<sub>4</sub>); 142° ((C5)<sub>2</sub>PbCl<sub>4</sub>); 141° ((C4)<sub>2</sub>PbCl<sub>4</sub>); 147° ((C6)<sub>2</sub>PbBr<sub>4</sub>); 147° ((C5)<sub>2</sub>PbBr<sub>4</sub>); 143° ((C4)<sub>2</sub>PbBr<sub>4</sub>)) and similar out-of plane distortions ((maximum angle of 10° ((C6)<sub>2</sub>PbCl<sub>4</sub>); 9° ((C5)<sub>2</sub>PbCl<sub>4</sub>); 15° ((C4)<sub>2</sub>PbCl<sub>4</sub>); 13° ((C6)<sub>2</sub>PbBr<sub>4</sub>); 11° ((C5)<sub>2</sub>PbBr<sub>4</sub>); 12° ((C4)<sub>2</sub>PbBr<sub>4</sub>)). The emission properties of the three chloride compounds on one side and the three bromide compounds on the other side are similar: broad band type but weak intensity for the chloride series, main narrow excitonic band and strong intensity for the bromide series (see photos/Figure 2 and “Luminescence properties” section). As already highlighted,<sup>26</sup> this shows that the nature of halides has a main impact on emission properties of halide perovskites, chloride compounds usually giving broad band emission of weak intensity at room temperature.

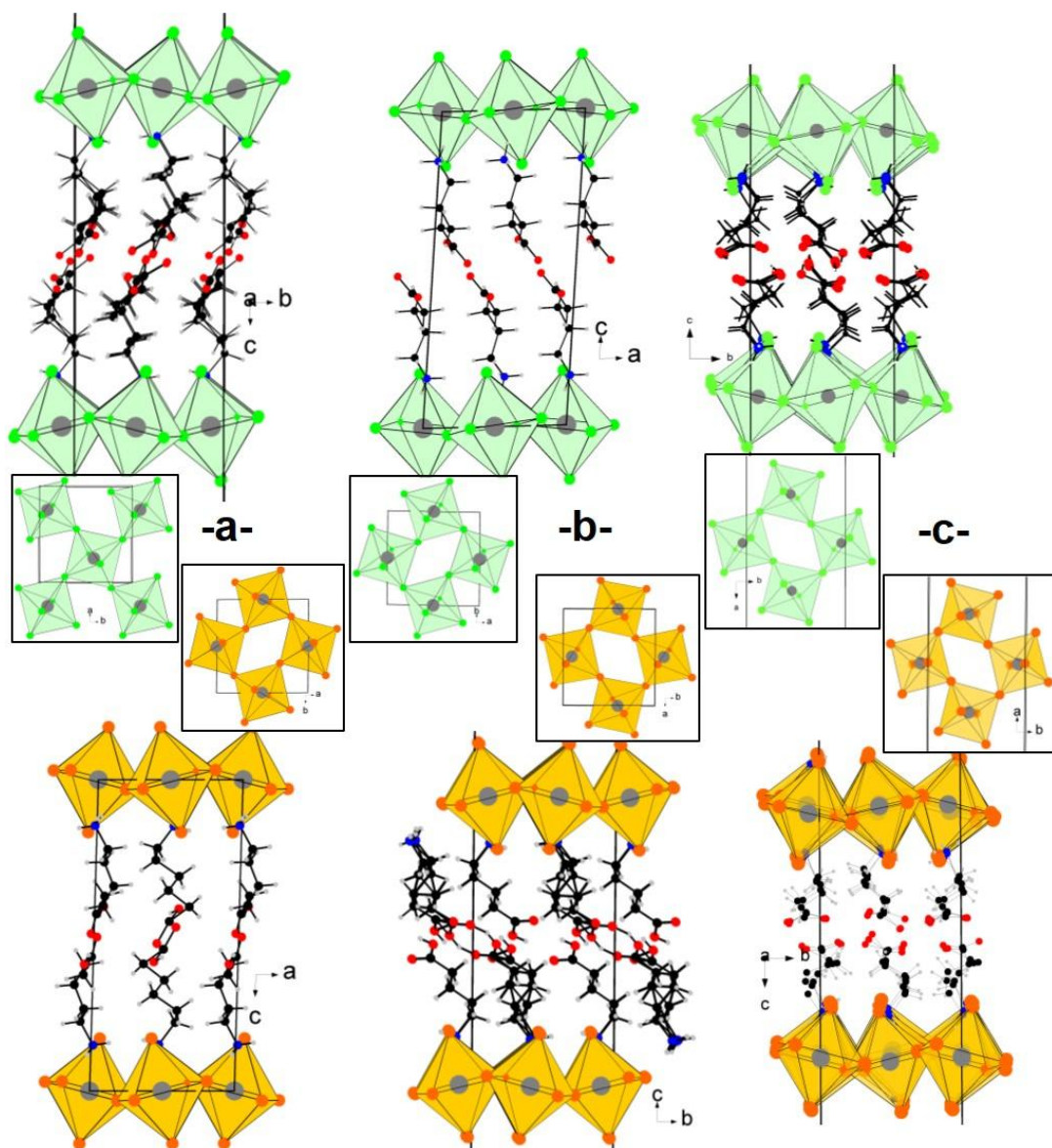


**Figure 2.** Structures of the layered perovskites  $(C_n)_2PbX_4$ : (a)  $n=6$ ,  $X= Cl$  (up) and  $X= Br$  (down); (b)  $n=5$ ,  $X= Cl$  (up) and  $X= Br$  (down); (c)  $n=4$ ,  $X= Cl$  (up) and  $X= Br$  (down). General view along the layers planes and view of a  $PbX_4^{2-}$  perovskite layer allowing to estimate the out-of-plane and in-plane distortions, respectively.

### **Mixed organic cations and mixed halides solid solutions.**

The presence of two kinds of cations in the interlayer space of 2D perovskites, if well known in the field of layered oxide perovskites,<sup>30</sup> is rare in the field of hybrid perovskites. The first structure incorporating two kinds of organic cations is (5FPEA,NEA)SnI<sub>4</sub> (NEA<sup>+</sup>: 2-naphthylenethylammonium, 5FPEA<sup>+</sup>: 2,3,4,5,6-pentafluorophenethylammonium).<sup>31</sup> More recently, some other examples have been reported such as (Cs)(Gua)[PbX<sub>4</sub>] (X = Br, I) and (Cs)(Gua)[CsPb<sub>2</sub>Br<sub>7</sub>] (Gua = guanidinium),<sup>32</sup> or (Gua,MA)[(MA)<sub>n-1</sub>Pb<sub>n</sub>I<sub>3n+1</sub>] (n = 1, 2, 3; MA<sup>+</sup>: methylammonium).<sup>33</sup>

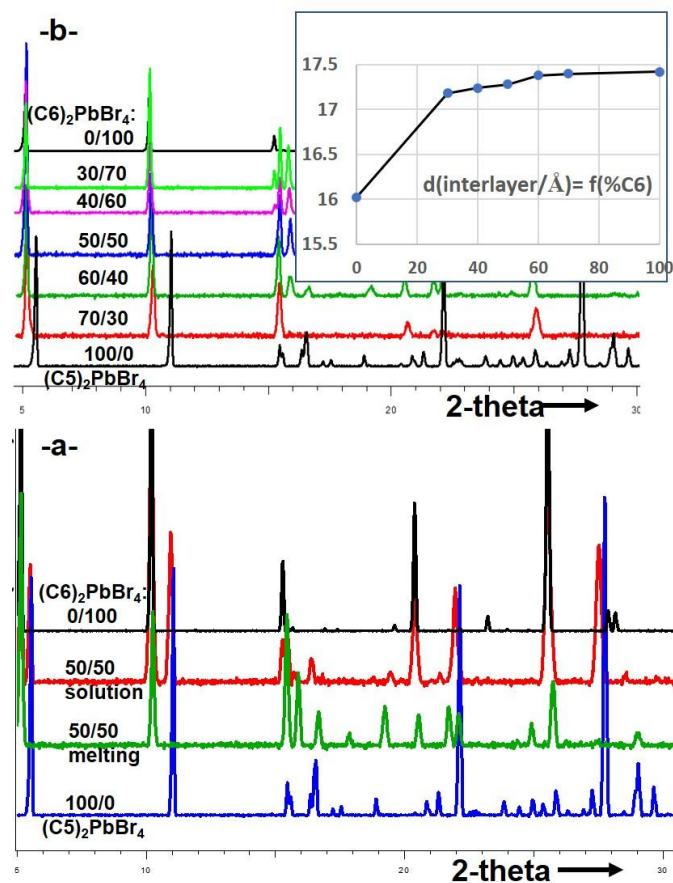


**Figure 3.** a) PXRD patterns of reagents  $(C5)_2PbBr_4$  and  $(C6)_2PbBr_4$  and of powders obtained by a molten state process (“50/50 - melting”) or a solution synthesis (“50/50 – solution”) from reagents in 1/1 ratio; b) PXRD patterns of the solid solution  $(C6_{1-x}C5_x)_2PbBr_4$  from  $x=0$  (upper pattern, 100% of C6) to  $x=1$  (lowest pattern, 100% of C5) obtained by the molten state process. In the inset, evolution of the interlayer distance along with the percentage of C6 (=  $(C6/(C5+C6)) \times 100$ ).

The main synthetic route used to prepare solid solutions, mainly mixed halide compounds in the field of halide perovskites, is the solution coprecipitation method. Such experiment has been carried out starting from  $(C5)_2PbBr_4$  and  $(C6)_2PbBr_4$  (1/1 ratio) in order to obtain the mixed organic compound  $(C5_{0.5}C6_{0.5})_2PbBr_4$ . The PXRD pattern of the obtained solid is shown Figure 3a clearly indicating that both  $(C5)_2PbBr_4$  and  $(C6)_2PbBr_4$  compounds are recrystallized as underlined by double peaks of typical (00l) lines at low 2-theta angles (around  $5.5^\circ$  and  $10.5^\circ$ ). In contrast, when a powder containing both compounds in 1/1 ratio is heated beyond melting for one to two minutes, the liquid being stirred during this time, and recrystallized upon cooling, a single phase is obtained as underlined by single (00l) lines at low angles (Figure 3a). This demonstrates the great interest of this solvent-free synthetic process in the molten state that can lead to new compounds/compositions which could not be obtained via a classical synthesis in solution. Using this molten state process, we explored the solid solutions  $(C5_{1-x}C6_x)_2PbBr_4$ ,  $(C4_{1-x}C5_x)_2PbBr_4$  and  $(C4_{1-x}C6_x)_2PbBr_4$ . The Figure 3b (see also Figure S15) shows PXRD patterns of several compositions in the C5/C6 system, from  $x=0$  (100% of C5) to  $x=1$  (100% of C6) through  $x=0.3$  (70%C5/30%C6), 0.4, 0.5, 0.6 and 0.7. The X-ray lines at  $5-5.5^\circ$  and  $10-11^\circ$  are directly related to the interlayer distance  $d_{inter}$  ( $d(5-5.5^\circ) = d_{inter}$ ) and we clearly see that  $d_{inter}$  is greater for  $(C6)_2PbBr_4$  than for  $(C5)_2PbBr_4$  (line at lower angle for the C6 compound) as expected for a compound based on a longer organic cation. The single lines at  $5.5^\circ$  and  $10.5^\circ$  for all intermediate compositions indicate that a single phase is obtained, meaning a full composition range for this solid solution. Interestingly, as underlined by the graph  $d_{inter} = f(\%C6)$ , it appears that as soon as C6 is added in the system, for instance for  $x=0.3$ , the corresponding interlayer distance roughly corresponds to the one of  $(C6)_2PbBr_4$  meaning that the longer cation imposes the interlayer distance (Figure 3b-inset-). For both the  $(C4_{1-x}C5_x)_2PbBr_4$  and  $(C4_{1-x}C6_x)_2PbBr_4$

systems, the range of existence is  $0 < x \leq 0.5$ . This is clearly deduced from PXRD pattern which show single lines around  $5.2-5.5^\circ$  and  $11-12^\circ$  for  $x = 0.2$  to  $x = 0.5$  while double lines are observed for  $0.5 < x < 1$  indicating the presence of two phases for these last compositions (Figure 4 and Figure S16 -C4/C5 system-). Moreover, in contrast with the C5/C6 system, on one hand there is a continuous shift of the two first lines to low angles as  $x$  increases from 0.2 to 0.5 (Figures 4 and S16), and on the other hand, the interlayer distance of structures containing the same quantity of both cations  $-(C_{4.5}C_{6.5})_2PbBr_4$  ( $d_{inter} = 15.92 \text{ \AA}$ ) or  $(C_{4.5}C_{5.5})_2PbBr_4$  ( $d_{inter} = 15.32 \text{ \AA}$ )- is intermediate between the distance of the two parent compounds ( $14.20 \text{ \AA}$  (C4),  $16.02 \text{ \AA}$  (C5),  $17.42 \text{ \AA}$  (C6)) (see also Figure S17:  $d_{inter} = f(\%C5 \text{ or } C6)$ ). This is a good indication that pairs of hydrogen bonding cations C4-C6 (or C4-C5) are created in the interlayer space. A structural model is proposed for  $(C_{4.5}C_{6.5})_2PbBr_4$  in Figure 4.

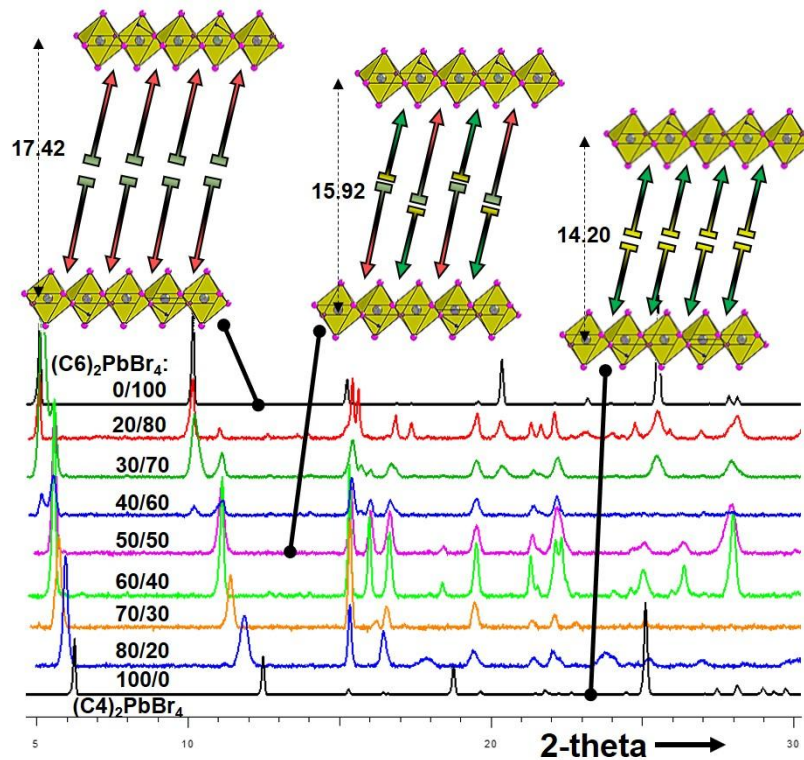


**Figure 4.** PXRD patterns of the solid solution  $(C_{6_{1-x}}C_{4_x})_2PbBr_4$  from  $x=0$  (100% bromide perovskite) to  $x=1$  (100% chloride perovskite). The  $0.5 < x < 1$  compositions lead to a mixture of phases as highlighted by double peaks around  $5.5^\circ$  and  $11^\circ$ . In the upper part are shown structural models corresponding to the C4-based perovskite ( $d(\text{interlayer})=14.2 \text{ \AA}$ ), C6-based perovskite ( $d(\text{interlayer})=17.42 \text{ \AA}$ ) and mixed organic cations  $(C_{6_{0.5}}C_{4_{0.5}})_2PbBr_4$  ( $d(\text{interlayer})=15.92 \text{ \AA}$ ).

Mixed halide perovskites  $(A)_2Pb(X_{1-x}X'_x)_4$  have previously been prepared by solution coprecipitation methods for  $A=BA^+$  (buthylammonium),  $PMA^+$  (phenylmethylammonium),  $PEA^+$  (phenylethylammonium),<sup>34</sup>  $Br\text{-}PEA^+$  (4-bromo-phenylethylammonium),<sup>35</sup> or  $BZA^+$  (benzylammonium).<sup>36</sup> While different characterizations are necessary to check that the solid state phase has a composition close to the composition in solution, different compositions covering the full range from  $x=0$  to  $x=1$  are usually obtained. The molten state synthetical process, in addition to being solvent-free, allows a predictable fine control of the composition of compounds. We explored in this study the solid solutions  $(C_n)_2Pb(Br_{1-x}Cl_x)_4$  ( $n=4, 5, 6$ ;  $x=0, 0.25, 0.50, 0.75, 1$ ). For the three series (C4, C5 and C6), PXRD patterns show that single phases are obtained for all compositions indicating full ranges of existence (Figure 5 and Figure S18). As observed in other

such systems,  $d_{inter}$  of the  $(Cn)_2PbCl_4$  structure is comparable or slightly greater than  $d_{inter}$  of the  $(Cn)_2PbBr_4$  structure (14.24 Å vs 14.20 Å for C4, 16.70 Å vs 16.02 Å for C5 and 18.10 Å vs 17.42 Å for C6). This is explained by the fact that the substitution of Br by Cl in equatorial planes involves a change of the molecular organization in the interlayer space, as molecules tend to align perpendicularly to the inorganic layers. Thus, we observe that the angle between the perpendicular line to perovskite layers and the molecular axis of  $[C5..C5]^{2+}$  dimers increases from 40° for the chloride compound to 45° for the bromide compound (Figure S19). In the case of the  $(C6)_2Pb(Br_{1-x}Cl_x)_4$  series, there is a continuous increase of the  $c$  parameter (shift of (00l) lines to low angles) together with a continuous decrease of the  $a$  and  $b$  parameters (shift of (hk0) or (hkl) lines to high angles) when  $x$  increases (Figure 5a and Figure S20). This certainly means that, as usually observed, the substitution of Br by Cl on both equatorial and apical positions is of statistical type. The case of the solid solution  $(C5)_2Pb(Br_{1-x}Cl_x)_4$  is different. As observed in Figure 5b, the PXRD pattern of the  $x=0.25$  compound is comparable to the  $x=0$  one (100% bromide), while those of  $x=0.50$  and  $x=0.75$  are comparable to the  $x=1$  one (100% chloride). This is clearly indicated by a shift of the (004) line to low angles (increasing of the  $c$  cell parameter, Figure S20) and the shift of the (110) line to high angles from  $x=0.25$  to  $x=0.50$  compositions. As the  $a$  and  $b$  parameters (perovskite plane) are related to the nature of equatorial halides, this certainly indicates that the Br to Cl substitution occurs on apical sites for  $x=0.25$  (hypothetical perovskite layer:  $PbCl_{apical}Br_{apical}Br_{2(equatorial)}$ ), and for  $x=0.50$  on equatorial sites (hypothetical perovskite layer:  $PbBr_{2(apical)}Cl_{2(equatorial)}$ ) (see Figure 5b).

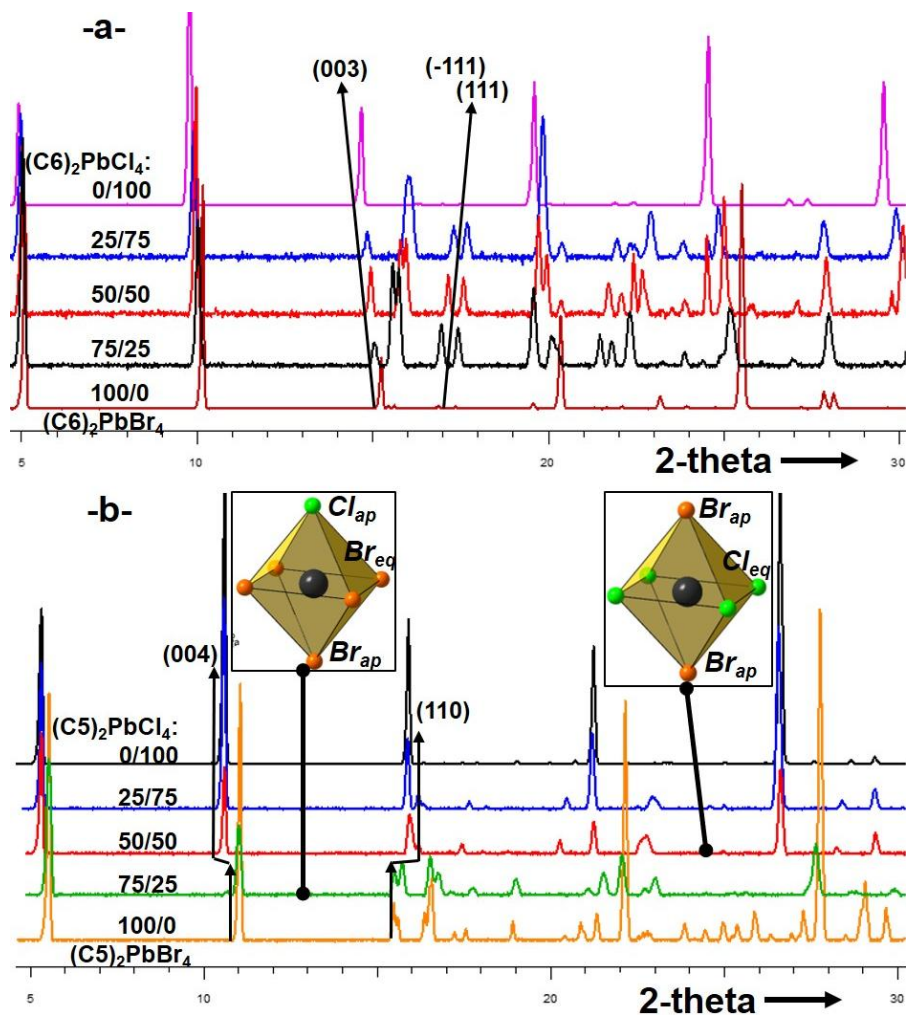


**Figure 5.** PXRD patterns of the solid solution  $(C6)_2Pb(Br_{1-x}Cl_x)_4$  -a- and  $(C5)_2Pb(Br_{1-x}Cl_x)_4$  -b- for  $x=0$  (100% bromide perovskite) to  $x=1$  (100 % chloride perovskite). In -a-, the evolution of (003), (-111) and (111) lines indicating an increase of  $c$  and decrease of  $a$  and  $b$  cell parameters along with  $x$  is undelined. In -b-, the abrupt change of positions of (004) and (110) lines from  $x=0.25$  to  $x=0.50$  compositions is underlined revealing a change in perovskite layers (hypothetical  $Pb(X,X')_6$  octahedra are drawn for these two compositions).

The case of the solid solution  $(C4)_2Pb(Br_{1-x}Cl_x)_4$  appears quite comparable to  $(C4)_2Pb(Br_{1-x}Cl_x)_4$  even if no significant change of the first two lines is observed (Figure S18) indicating that the interlayer spacing is here independent of the ratio Br/Cl (Figure S20). For  $x=0.25$  (75% bromine) the XRD pattern is comparable to that of the completely brominated compound with a slight shift of the (004) line towards low angles, whereas the  $x=0.50$  and  $x=0.75$  compositions have an XRD pattern quite comparable to that of the chlorinated compound.

DSC experiments of intermediate compositions of both solid solutions  $(Cn_{1-x}Cn'_x)_2PbBr_4$  and  $(Cn)_2Pb(Br_{1-x}Cl_x)_4$  have been carried out. For the mixed organic cations series, it appears that melting temperatures increase continuously when the length of the carbon chain increases (Figure S21). The situation is different for solid solutions involving both types of halides. This is especially spectacular for the  $(C4)_2Pb(Br_{1-x}Cl_x)_4$  series (Figure 6). While  $T_m$  is about 145 °C for the chloride and bromide compounds ( $x=0, 1$ ),  $T_m$  falls to 111°C and even 94 °C for  $x=0.50$  and  $x=0.75$ , respectively. The recrystallization temperature is also much lowered, by 50°C (from 130 °C ( $x=0, 1$ ) to 80 °C ( $x=0.75$ )). While less marked, a similar behavior is observed for the C5 and C6 series (Figures S22-23).

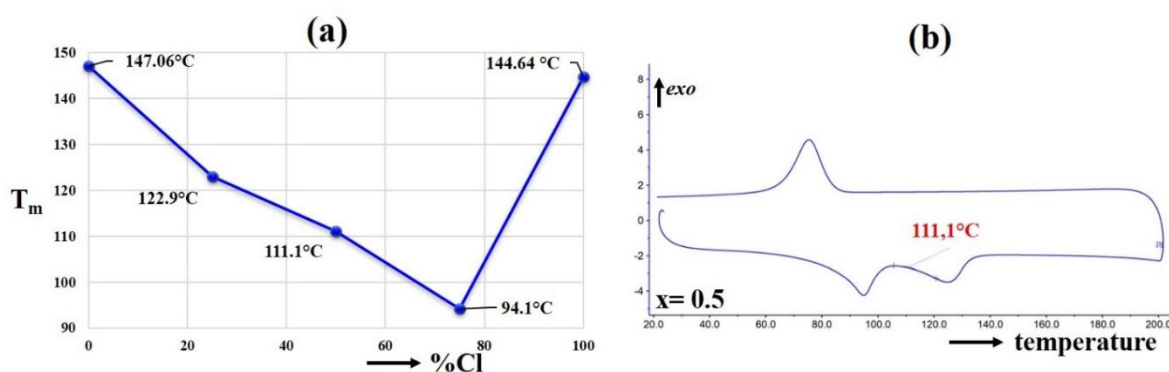


**Figure 6.** Evolution of the melting temperatures ( $T_m$ ) of  $(C4)_2Pb(Br_{1-x}Cl_x)_4$  along with 100x (= %Cl) (a); and DSC of the  $x=0.5$  composition (b).

### Luminescence properties.

The bromide perovskites  $(Cn)_2PbBr_4$  ( $n= 4-6$ ) display a bright white emission under UV lamp irradiation. Their emission spectra are similar, consisting of a narrow peak around 410 nm superimposed to a broad band extending to 650 nm, as often observed for such bromide layered perovskites (Figure 7a). As well known,<sup>7</sup> the high energy peak is assigned to the emission of free excitons (FE), while the broad band emission is usually attributed to self-trapped excitons (STE

states).<sup>4,5,25</sup> The excitation spectra (PLE) of both emissions are similar indicating a same origin. They consist of a narrow peak around 400 nm and a broad band centered at about 365 nm (Figure 7a). Due to a main blue component at 410 nm, these materials are finally far from ideal white emission (for instance the chromaticity coordinates are (0.22, 0.22) for (C4)<sub>2</sub>PbBr<sub>4</sub> vs (0.33, 0.33) for neutral white emitters). By partially substituting C<sub>n</sub> cations in (C<sub>n</sub>)<sub>2</sub>PbBr<sub>4</sub> perovskites by C<sub>n'</sub> cations ( $n' \neq n$ ) thanks to the molten state solvent-free synthetic process, structural modifications at the organic-inorganic interface and consequently of the inorganic network were expected, which could potentially lead to an increase of the STE component. However, no significant changes of the luminescence properties of intermediate compositions for the three solid solutions (C<sub>n</sub><sub>1-x</sub>C<sub>n'</sub><sub>x</sub>)<sub>2</sub>PbBr<sub>4</sub> ( $n, n' = 4, 5, 6$ ) compared to (C<sub>n</sub>)<sub>2</sub>PbBr<sub>4</sub> ( $n = 4, 5, 6$ ) compounds (Figure S24) could be observed. On Figure 7b are reported PL and PLE spectra of  $x = 0.5$  compounds ((C<sub>4.5</sub>C<sub>5.5</sub>)<sub>2</sub>PbBr<sub>4</sub>, (C<sub>4.5</sub>C<sub>6.5</sub>)<sub>2</sub>PbBr<sub>4</sub> and (C<sub>5.5</sub>C<sub>6.5</sub>)<sub>2</sub>PbBr<sub>4</sub>) which can be compared to those of bromide perovskites based on one type of organic cation (Figure 7a). We observe that the emission properties of solid solution based on C4 and C6 organic cation undergo the most important changes, with an increase of the I(STE)/I(FE) ratio from the all C4 compound to the (C<sub>4.5</sub>C<sub>6.5</sub>)<sub>2</sub>PbBr<sub>4</sub> compound. This composition corresponds to the upper limit of the existence range of this solid solution ( $0 \leq x \leq 0.5$ ) which may indicate a limit structure with distorted perovskite layers leading to the observed increasing of the STE component.

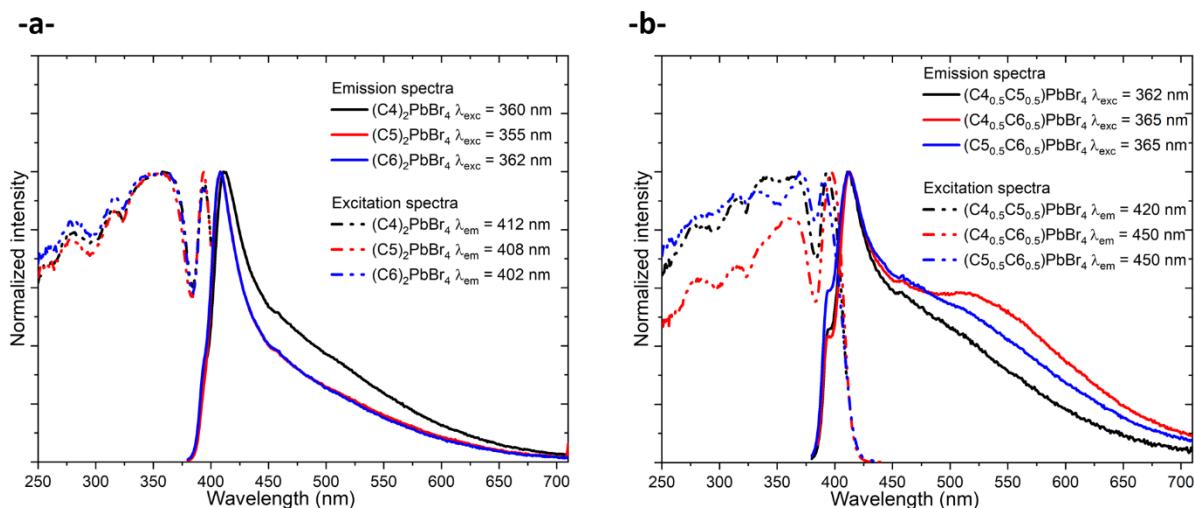


**Figure 7.** PL (full lines) and PLE (dotted lines) spectra of  $(C_n)_2PbBr_4$  ( $n = 4, 5, 6$ ) (a), and of solid solutions  $(C_{n_0.5}C_{n'0.5})_2PbBr_4$  (red:  $n = 4, n' = 6$ ; blue:  $n = 5, n' = 6$ ; black:  $n = 4, n' = 5$ ) (b).

Chloride perovskites are known for their greater potential than brominated phases to have broadband type emission properties.<sup>29</sup> For the three solid solutions  $(C_n)_2Pb(Br_{1-x}Cl_x)_4$  ( $n = 4-6$ ) studied here, the addition of chloride (increasing  $x$ ) involves the increasing of the STE component. The case of the  $(C4)_2Pb(Br_{1-x}Cl_x)_4$  series is reported in Figure 8a. For the  $x = 0.25$  composition, the FE peak is still present while the STE component increases compared to the  $x = 0$  composition (bromide compound). We also observe a blue shift of both FE emission and corresponding PLE peaks from  $x = 0$  to  $x = 0.25$ . This trend, known for such mixed halide perovskites, is explained by a decrease of the band valence level when the quantity of chlorides, more ionic than bromides, increases,<sup>7</sup> and consequently an increasing of the associated excitonic energy. When  $x = 0.75$ , only the broad band is observed as for the all chloride perovskite ( $x = 1$ ). The evolution of the chromaticity coordinates of the four compounds is reported on Figure 8b. We can observe an evolution from blue for  $x = 0$  (CIE coordinates of (0.22,0.22)) to yellow emission for the Cl-rich materials ((0.38,0.42) and (0.42,0.45) for  $x = 0.75$  and  $x = 1$  respectively) passing by whitish emission for  $x = 0.25$  (CIE coordinates of (0.27,0.31)), quite close to the ideal

white emitter (coordinates of (0.33, 0.33)). Their photoluminescence quantum efficiency (PLQE) is weak for the yellow emitters (1% and < 1% for  $x= 0.75$  and  $x= 1$ , respectively) and moderate for the Br-rich perovskites (PLQE of 8.7 % and 3.8 % for  $x= 0$  and  $x= 0.25$ , respectively). The detrapping from STE to FE, activated at different temperatures depending on the halogen, well explain this trend. In Br-rich materials, the FE is more intense because the detrapping is allowed at room temperature, contrary to Cl-rich materials where this detrapping process is not efficient at this temperature.<sup>29</sup> The emission properties of the two other solid solutions ( $(C5)_2Pb(Br_{1-x}Cl_x)_4$ ) and ( $(C6)_2Pb(Br_{1-x}Cl_x)_4$ ) are reported in Figure S25. Same trends are observed when  $x$  increases (increasing of the  $I(STE)/I(FE)$  ratio, blue shift of FE emission peaks together with peaks of the PLE spectra, decreasing of the emission intensities). However, we notice unusual emission properties of both chloride perovskites  $(C5)_2PbCl_4$  and  $(C6)_2PbCl_4$  as well as  $(C6)_2Pb(Br_{0.25}Cl_{0.75})_4$ . A broad band emission centered around 410 nm ( $C5$ ,  $x= 1$ ), 450 nm ( $C6$ ,  $x= 1$ ) and 465 nm ( $C6$ ,  $x= 0.75$ ) is observed in the PL spectra, while PLE spectra consist of a single peak at 365 nm ( $C6$  and  $C5$ ,  $x= 1$ ) or 388 nm ( $C6$ ,  $x= 0.75$ ). Figure S26 reports the PL and PLE spectra of chloride salts of organic cations,  $C_nCl$  ( $n= 4, 5, 6$ ). The shape and peak positions of emission bands (centered around 430 nm) and excitation bands (in the range 350-360 nm) corresponds well to the one observed for the  $C5$  and  $C6$ -based Cl-perovskites, meaning that emission properties of these two compounds certainly originate from the organic components.

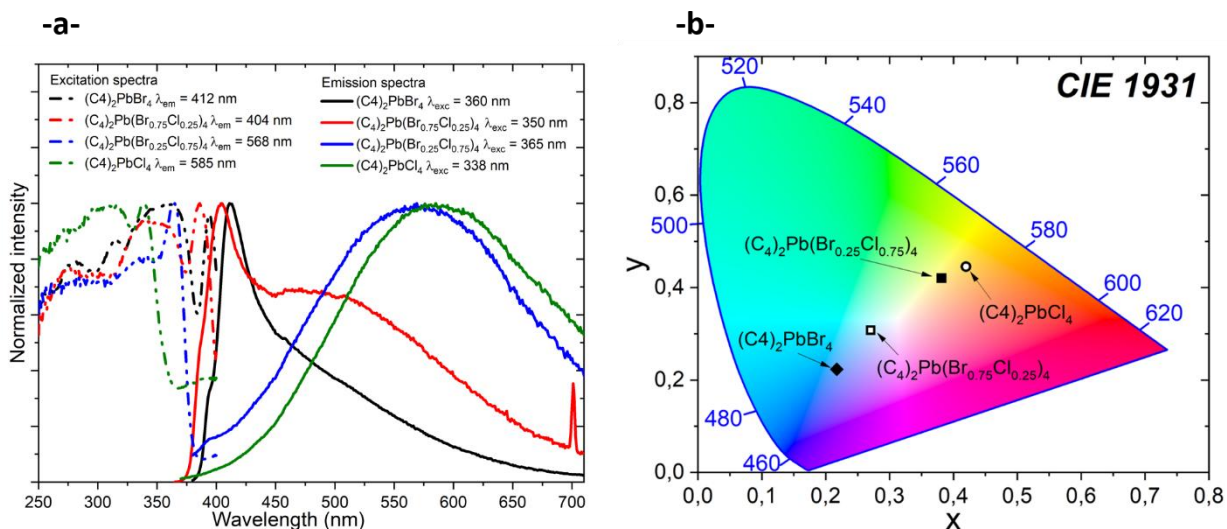


**Figure 8.** PL and PLE spectra of the solid solution  $(C_4)_2Pb(Br_{1-x}Cl_x)_4$  (a), and corresponding chromaticity diagram (b).

## CONCLUSION

The work reported here illustrates one of the opportunities offered when hybrid perovskites present a congruent melting (melting without decomposition): to carry out chemistry in the molten state in order to obtain original phases which couldn't be accessible from solution routes. Starting from halide perovskites of  $(Cn)_2PbX_4$  type ( $Cn = NH_3^+-(CH_2)_{n-1}-COOH$ ,  $n = 4, 5, 6$ ;  $X = Br, Cl$ ) exhibiting congruent melting (at  $T_m$  in the  $130^\circ C-200^\circ C$  range), the solid solutions  $(Cn_{1-x}Cn'_x)_2PbBr_4$  and  $(Cn)_2Pb(Br_{1-x}Cl_x)_4$  have been prepared by a solvent-free process, in the molten state. Mixed halide perovskites have been previously prepared using a co-precipitation method, but a solid solution incorporating two different organic cations had never been prepared.

Moreover halide substitutions strongly impacts the thermal properties, lowering  $T_m$  down to 100 °C for  $(C4)_2Pb(Br_{0.25}Cl_{0.75})_4$  which constitutes a record in the field of halide perovskites. The bromide perovskites  $(Cn)_2PbBr_4$ , ( $n = 4, 5, 6$ ) display quite strong withish luminescence properties consisting of a main blue component. Substitutions on organic sites or halide sites provide opportunities to tune the emission properties of these hybrids. The strategy of incorporating two organic cations into the brominated perovskites did not lead to significant modification of the emission properties, probably indicating that few structural modifications take place. In the case of mixed halide compounds, the emission properties are greatly modified mainly due to the nature of halides: on one hand, the incorporation of chlorides leads to emission bands in the all visible region, but in the other hand a decrease of emission intensities is observed. The composition which present the best compromise (CIE coordinates approaching (0.33, 0.33) and high emission intensities), corresponds to  $x= 0.25$ , especially in the case of C4-based perovskites.

#### ASSOCIATED CONTENT

**Supporting Information.** The following files are available free of charge.

Experimental details for synthesis, XRD characterizations, DSC curves, structural analysis, PL and PLE spectra.

X-ray crystallographic data of  $(Cn)_2PbX_4$  ( $n= 6, X= Br$ ;  $n= 6, X= Cl$ ;  $n= 4, X= Cl$ ).

#### AUTHOR INFORMATION

##### Corresponding Author

\*nicolas.mercier@univ-angers.fr

## Author Contributions

The manuscript was written through contributions of all authors. All authors have given approval to the final version of the manuscript.

## Notes

The authors declare no competing financial interest.

## ACKNOWLEDGMENT

This work is supported by the regional EUR LUMOMAT consortium (MeltHP project). We warmly thank Dr Tobias Stürzer, senior application scientist in the Bruker AXS Application Laboratory at Karlsruhe (Germany), for the X-ray data collection of  $(C6)_2PbCl_4$ .

## REFERENCES

- (1) Jena, A. K.; Kulkarni, A.; Miyasaka, T. Halide Perovskite Photovoltaics: Background, Status, and Future Prospects. *Chem. Rev.* **2019**, *119*, 3036-3103
- (2) Turren-Cruz, S.-H.; Hagfeldt, A.; Saliba, M. Methylammonium-free, high-performance, and stable perovskite solar cells on a planar architecture. *Science* **2018**, *362*, 449-453.
- (3) Gratzel, M. The Rise of Highly Efficient and Stable Perovskite Solar Cells. *Acc. Chem. Res.* **2017**, *50*, 487-491.
- (4) Smith, M. D.; Connor, B. A.; Karunadasa, H. I. Tuning the luminescence of layered halide perovskites. *Chem. Rev.* **2019**, *119*, 3104-3139.
- (5) Cortecchia, D.; Yin, J.; Petrozza, A.; Soci, C. White light emission in low-dimensional perovskites. *J. Mater. Chem. C* **2019**, *7*, 4956-4969.

- (6) Mao, L.; Guo, P.; Kepenekian, M.; Hadar, I.; Katan, C.; Even, J.; Schaller, R. D.; Stoumpos, C. C.; Kanatzidis, M. G. Structural Diversity in White-Light-Emitting Hybrid Lead Bromide Perovskites. *J. Am. Chem. Soc.* **2018**, *140*, 13078–13088.
- (7) Mitzi D. B., Prog. Inorg. Chem. (Ed. Karlin, K. D.), John Wiley & Sons, Inc.: Hoboken, NJ, USA, **1999**; pp 1–121.
- (8) Saparov, B.; Mitzi, D. B. Organic-Inorganic Perovskites: Structural Versatility for Functional Materials Design. *Chem. Rev.* **2016**, *116*, 4558–4596.
- (9) Mercier, N. Hybrid Halide Perovskites: Discussions on Terminology and Materials. *Angew. Chemie Int. Ed.* **2019**, *58*, 17912-17917.
- (10) Ren, H.; Yu, S.; Chao, L.; Xia, Y.; Sun, Y.; Zuo, S.; Li, F.; Niu, T.; Yang, Y.; Ju, H.; Li, B.; Du, H.; Gao, X.; Zhang, J.; Wang, J.; Zhang, L.; Chen, Y.; Huang, W. Efficient and stable Ruddlesden–Popper perovskite solar cell with tailored interlayer molecular interaction. *Nat. Photonics* **2020**, *14*, 154–163.
- (11) Liang, C.; Gu, H.; Xia, Y.; Wang, Z.; Liu, X.; Xia, J.; Zuo, S.; Hu, Y.; Gao, X.; Hui, W.; Chao, L.; Niu, T.; Fang, M.; Lu, H.; Dong, H.; Yu, H.; Chen, S.; Ran, X.; Song, L.; Li, B.; Zhang, J.; Peng, Y.; Shao, G.; Wang, J.; Chen, Y.; Xing, G.; Huang, W. Two-dimensional Ruddlesden–Popper layered perovskite solar cells based on phase-pure thin films. *Nat. Energy* **2021**, *6*, 38-45
- (12) Li, X.; Hoffman, J. M.; Kanatzidis, M. G. The 2D Halide Perovskite Rulebook: How the Spacer Influences Everything from the Structure to Optoelectronic Device Efficiency. *Chem. Rev.* **2021**, *121*, 2230–2291.
- (13) Mitzi, D. B. Synthesis, crystal structure, and optical and thermal properties of (C<sub>4</sub>H<sub>9</sub>NH<sub>3</sub>)<sub>2</sub>MI<sub>4</sub> (M=Ge, Sn, Pb). *Chem. Mater.* **1996**, *8*, 791-800

- (14) Smith, M. D.; Karunadasa, H. I. White-Light Emission from Layered Halide Perovskites. *Accounts of Chemical Research* **2018**, *51*, 619-627
- (15) Yangui, A.; Garrot, D.; Lauret, J. S.; Lusson, A.; Bouchez, G.; Deleporte, E.; Pillet, S.; Bendeif, E. E.; Castro, M.; Triki, S.; Abid, Y.; Boukheddaden, K. Optical Investigation of Broadband White-Light Emission in Self-Assembled Organic-Inorganic Perovskite (C<sub>6</sub>H<sub>11</sub>NH<sub>3</sub>)(<sub>2</sub>)PbBr<sub>4</sub>. *J Phys Chem C* **2015**, *119*, 23638-23647
- (16) B. A. Rosalesa, L. Weia, J. Vela. Synthesis and mixing of complex halide perovskites by solvent-free solid-state methods. *J. of Solid. State Chem.* **2019**, *271*, 206-215
- (17) Petrov, A. A.; Belich, N. A.; Grishko, A. Y.; Stepanov, N. M.; Dorofeev, S. G.; Maksimov, E. G.; Shevelkov, A. G.; Zakeeruddin, S. M.; Graetzel, M.; Tarasov, A. B.; Goodilin, E. A. A new formation strategy of hybrid perovskites via room temperature reactive polyiodide melts. *Mater. Horiz.* **2017**, *4*, 625-632
- (18) Leupold, N.; Panzer, F. Recent Advances and Perspectives on Powder-Based Halide Perovskite Film Processing. *Adv. Funct. Mater.* **2021**, *31*, 2007350.
- (19) Mitzi, D. B.; Medeiros, D. R.; DeHaven, P. W. Low-Temperature Melt Processing of Organic– Inorganic Hybrid Films. *Chem. Mater.* **2002**, *14*, 2839-2841.
- (20) Li, T.; Dunlap-Shohl, W. A.; Han, Q.; Mitzi, D. B. Melt processing of hybrid organic– inorganic lead iodide layered perovskites. *Chem. Mater.* **2017**, *29*, 6200-6204.
- (21) Li, T.; Dunlap-Shohl, W. A.; Reinheimer, E. W.; Le Magueres, P.; Mitzi, D. B. Melting temperature suppression of layered hybrid lead halide perovskites via organic ammonium cation branching. *Chemical Science* **2019**, *10*, 1168-1175.

- (22) Ben Haj Salah, M.; Mercier, N.; Dabos-Seignon, S.; Botta, C. Solvent-Free Preparation and Moderate Congruent Melting Temperature of Layered Lead Iodide Perovskites for Thin-Film Formation. *Angew. Chem. Int. Ed.* **2022**, e202206665. doi.org/10.1002/anie.202206665
- (23) Zhou, G.; Jiang, X.; Molokeev, M.; Lin, Z.; Zhao, J.; Wang, J.; Xia, Z. Optically Modulated Ultra-Broad-Band Warm White Emission in Mn<sup>2+</sup>-Doped (C<sub>6</sub>H<sub>18</sub>N<sub>2</sub>O<sub>2</sub>)PbBr<sub>4</sub> Hybrid Metal Halide Phosphor. *Chem. Mater.* **2019**, *31*, 5788-5795.
- (24) Zhou, G.; Su, B.; Huang, J.; Zhang, Q.; Xia, Z. Broad-band emission in metal halide perovskites: Mechanism, materials, and applications. *Materials Science & Engineering R* **2020**, *141*, 100548
- (25) Smith, M. D.; Jaffe, A.; Dohner, E. R.; Lindenberg, A. M.; Karunadasa, H. I. Structural origins of broadband emission from layered Pb–Br hybrid perovskites. *Chemical Science* **2017**, *8*, 4497-4504.
- (26) Ben Haj Salah, M.; Mercier, N.; Dittmer, J.; Zouari, N.; Botta, C. The Key Role of the Interface in the Highly Sensitive Mechanochromic Luminescence Properties of Hybrid Perovskites. *Angew. Chemie Int. Ed.* **2021**, *60*, 834-839
- (27) Krummer, M.; Zimmermann, B.; Klingenberg, P.; Daub, M.; Hillebrecht, H. Perovskite- Related 2D Compounds in the System 5- Amino Valerian Acid Cation/MA/Pb/X (X= Cl, Br)–Synthesis, Crystal Structures, and Optical Properties. *Eur. J. of Inorg. Chem.* **2020**, *48*, 4581-4592.
- (28) Krause, L.; Herbst-Irmer, R.; Sheldrick, G.M.; Stalke, D. Comparison of silver and molybdenum microfocus X-ray sources for single-crystal structure determination. *J. Appl. Cryst.* **2015**, *48*, 3-10.

- (29) Gautier, R.; Paris, M.; Massuyeau, F. Exciton-self-trapping in hybrid lead halides: Role of halogen. *J. Am. Chem. Soc.* **2019**, *141*, 12619-12623.
- (30) Dion, M.; Ganne, M.; Tournoux, M. Nouvelles familles de phases M(I)M(II)2Nb3O10 a feuillets “perovskites”. *Materials Research Bulletin* **1981**, *16*, 1429-1435.
- (31) Xu, Z.; Mitzi, D. B. SnI4<sup>2-</sup>-based hybrid perovskites templated by multiple organic cations: Combining organic functionalities through noncovalent interactions. *Chem. Mater.* **2003**, *15*, 3632-3637.
- (32) Nazarenko, O.; Kotyrba, M. R.; Wörle, M.; Cuervo-Reyes, E.; Yakunin, S.; Kovalenko, M. V. Luminescent and photoconductive layered lead halide perovskite compounds comprising mixtures of cesium and guanidinium cations. *Inorg. Chem.* **2017**, *56*, 11552-11564.
- (33) Soe, C. M. M.; Stoumpos, C. C.; Kepenekian, M.; Traoré, B.; Tsai, H.; Nie, W.; Wang, B.; Katan, C.; Seshadri, R.; Mohite, A. D. New type of 2D perovskites with alternating cations in the interlayer space, (C(NH<sub>2</sub>)<sub>3</sub>)(CH<sub>3</sub>NH<sub>3</sub>)<sub>n</sub>PbnI<sub>3n+1</sub>: Structure, properties, and photovoltaic performance. *J. Am. Chem. Soc.* **2017**, *139*, 16297-16309.
- (34) Zhou, G.; Li, M.; Zhao, J.; Molochev, M. S.; Xia, Z. Single- Component White- Light Emission in 2D Hybrid Perovskites with Hybridized Halogen Atoms. *Adv. Opt. Mater.* **2019**, *7*, 1901335.
- (35) Pareja-Rivera, C.; Morán-Muñoz, J. A.; Gómora-Figueroa, A. P.; Jancik, V.; Vargas, B.; Rodríguez-Hernández, J.; Solís-Ibarra, D. Optimizing Broadband Emission in 2D Halide Perovskites. *Chem. Mater.* **2022**, *34*, 9344-9349.

- (36) Jung, M.-H. White-Light Emission from the Structural Distortion Induced by Control of Halide Composition of Two-Dimensional Perovskites ((C<sub>6</sub>H<sub>5</sub>CH<sub>2</sub>NH<sub>3</sub>)<sub>2</sub>PbBr<sub>4-x</sub>Cl<sub>x</sub>). *Inorg. Chem.* **2019**, *58*, 6748-6757.

## For Table of Contents Use Only

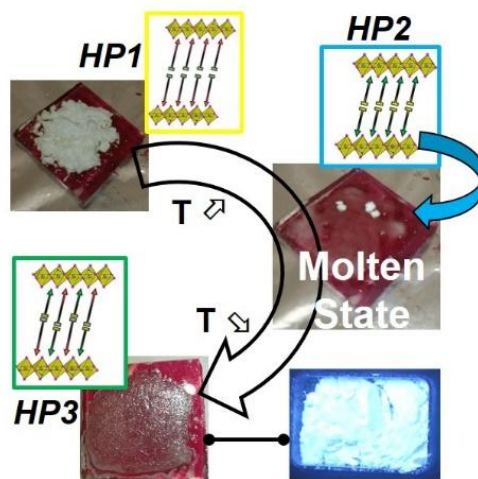
### Manuscript title

Chemistry in the Molten State: Opportunities for Designing and Tuning Emission Properties of Halide Perovskites.

### Authors

Feten Hleli, Nicolas Mercier,\* Maroua Ben Haj Salah, Magali Allain, Nabil Zouari, Florian Massuyeau, Romain Gautier

### TOC graphic



### SYNOPSIS.

Starting from halide perovskites of  $(Cn)_2PbX_4$  type ( $Cn = NH_3^+(CH_2)_{n-1}COOH$ ,  $n = 4, 5, 6$ ;  $X = Br, Cl$ ) exhibiting congruent melting (at  $T_m$  in the  $130^\circ C - 200^\circ C$  range), the solid solutions  $(Cn_{1-x}Cn'_x)_2PbBr_4$  and  $(Cn)_2Pb(Br_{1-x}Cl_x)_4$  have been prepared by a solvent-free process (synthesis in the molten state). The emission properties are slightly tuned in the case of mixed organic cations systems, whereas modifications are more dramatic in the case of mixed halides systems, leading to emission properties through the entire visible region.